

Molecular Dynamics Simulation of Cross-Linked Epoxy Polymers: the Effect of Force Field on the Estimation of Properties

B. Arab*, A. Shokuhfar†

Advanced Materials and Nanotechnology Research Lab, Faculty of Mechanical Engineering, Khajeh Nasir Toosi University of Technology, P.O. Box: 19395-1999 Tehran, Iran

(Received 27 January 2013; published online 28 March 2013)

In this paper, the molecular dynamics method was used to calculate the physical and mechanical properties of the cross-linked epoxy polymer composed of diglycidyl ether of bisphenol-A (DGEBA) as resin and diethylenetriamine (DETA) as curing agent. Calculation of the properties was performed using the constant-strain (static) approach. A series of independent simulations were carried out based on four widely used force fields; COMPASS, PCFF, UFF and Dreiding. Proper comparisons between the results and also with experimental observations were made to find the most suitable force field for molecular dynamics simulation of polymer materials.

Keywords: Cross linking, Epoxy polymers, Force field, Mechanical properties, Molecular dynamics.

PACS numbers: 31.15.at, 61.25.hp, 82.35.Lr

1. INTRODUCTION

Epoxyes with 3D cross-linked structures have superior properties, making them attractive materials for different applications including coatings, composite materials, adhesives, electronic packaging, etc. They are thermosetting polymers with linear or 3D cross-linked structures, typically obtained from reaction between epoxy resins and proper curing agents. The main parameters controlling the polymer structure are the functionality of monomers, the molar ratio between initiator and monomers, the concentration of species that are involved in chain transfer steps, and temperature (thermal cycle) that affects the relative rates of different steps [1]. Among them, the functionality of reactants, i.e. the number of reactive sites per monomer, determines whether the final structure of yielded polymer would be linear or cross-linked.

In recent years, few attempts have been made to study the dynamics of cross linking process and structure-property relationship of cross-linked polymers. Doherty et al. [2] developed a polymerization molecular dynamics scheme to construct cross-linked poly (methacrylates) (PMA) networks. By means of large-scale MD simulations, Tsige and Stevens [3] investigated the effect of cross-linker functionality and interfacial bond density on the fracture behavior of highly cross-linked polymer networks. Employing the MD method, the cross linking of poly (vinyl alcohol) (PVA) with polyol curing agent was simulated by Bermegjo and Ugarte [4, 5], and the material properties of the cross-linked polymer were calculated. Hölck et al. [6] studied the thermo-mechanical behavior of the polymer obtained from cross linking between epoxy phenol novolac (EPN) and bisphenol-A hardener. Some researchers studied the EPON 862 resin cross-linked with diethyltoluenediamine (DETDA) [7-11] and triethylenetetramine (TETA) [12-15] curing agents. Cross linking of DGEBA resin

with isophorone diamine (IPD) [16-19], trimethylene glycol di-p-aminobenzoate (TMAB) [20], DETDA [21], diamine [22], diaminodiphenyl sulfone (DDS) [23], methylenedianiline (MDA) [24], and poly(oxypropylene) (POP) diamines [25] were simulated and studied by some others.

The epoxy resin, diglycidyl ether of bisphenol-A (DGEBA) also known as EPON 828, can be cross-linked in presence of diethylenetriamine (DETA) curing agent to yield one of the frequently used epoxy polymers in structural composites and coatings. Molecular dynamics (MD) is utilized in this study to predict the properties of the cross-linked epoxy polymer using some of frequently used force fields.

2. MOLECULAR STRUCTURES OF DGEBA AND DETA

DGEBA is a bi-functional reactant with two *epoxide* groups, while DETA has five reactive sites including both primary and secondary *amine* groups and hence is a multi-functional (fivefold-functional) reactant. Therefore, DGEBA and DETA are able to produce 3D cross-linked epoxy polymers. The molecular structures of EPON 828 and DETA are represented in Fig. 1.

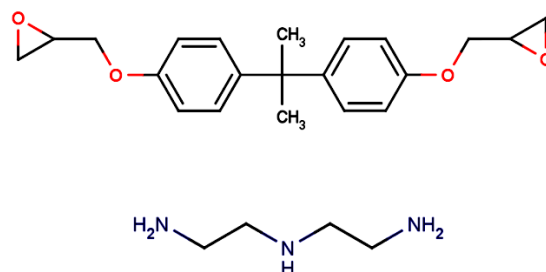


Fig. 1 – Molecular structures of EPON 828 (top), and DETA (bottom)

* arab@dena.kntu.ac.ir

† shokuhfar@kntu.ac.ir

The article was reported at the 2nd International Conference «Nanomaterials: Applications & Properties-2012»

Each DETA molecule can react at most with five DGEBA molecules, each of which capable of being connected to another DETA molecule through its opposite epoxide head. Thus, the ideal composition ratio of DGEBA/DETA in the blend is 5/2.

3. FORCE FIELDS

Modeling and simulations were performed using Materials Studio 5.5 software package [26]. The Condensed-phase Optimized Molecular Potentials for Atomistic Simulation Studies (COMPASS) [27-33], Polymer Consistent Force Field (PCFF) [28, 34-37], Universal Force Field (UFF) [38-40], and Dreiding [41] were utilized independently in four sets of molecular mechanics (MM) and dynamics (MD) simulations.

The PCFF and COMPASS are known as second generation or class II force fields. As members of consistent force fields family, they are parameterized against a wide range of organic compounds. PCFF is also applicable for polycarbonates, melamine resins, polysaccharides, inorganic materials, about 20 metals, as well as for carbohydrates, lipids, and nucleic acids.

COMPASS, as the new version of PCFF, is an ab-initio force-field parameterized for different molecules including most common organics, small inorganic molecules, and polymers to predict various properties of the materials [27, 29-33]. The total energy function in COMPASS force-field is composed of 12 terms including *valence* and *non-bonded interaction* terms [33]. Valence terms fall into two categories: *diagonal* (bond stretching, bending, torsion, and out-of-plane potentials), and *off-diagonal cross-coupling* terms (describing the interactions between diagonal terms). The non-bonded interactions, including relatively short range van der Waals (vdW) and long range electrostatic interactions, are described by Lennard-Jones (LJ) 9-6 and Coulombic functions, respectively.

UFF is a purely diagonal, harmonic forcefield, in which bond stretching and angle bending are described by harmonic and Fourier cosine expansion terms, respectively, while cosine-Fourier expansion terms are used for torsions and inversions. The vdW interactions are described by the Lennard-Jones potential. Electrostatic interactions are described by atomic monopoles and a screened (distance-dependent) Coulombic term. UFF has full coverage of the periodic table, and is relatively accurate for predicting geometries and conformational energy differences of organic molecules, main-group inorganics, and metal complexes. The atomic parameters are combined using a prescribed set of equations that generate forcefield parameters for bond, angle, torsion, out-of-plane, and van der Waals and Coulombic energy terms. Dummy atoms are used in complexation and are associated with explicit parameters [42].

General force constants and geometry parameters for the Dreiding forcefield are based on simple hybridization rules rather than on specific combinations of atoms. The Dreiding forcefield does not generate parameters automatically in the way that UFF does. Instead, explicit parameters were derived by a rule-based approach. The Dreiding forcefield is a purely diagonal forcefield with harmonic valence terms and a cosine-

Fourier expansion torsion term. The umbrella functional form is used for inversions, which are defined according to the Wilson out-of-plane definition. The van der Waals interactions are described by the Lennard-Jones potential. Electrostatic interactions are described by atomic monopoles and a screened (distance-dependent) Coulombic term. Hydrogen bonding is described by an explicit Lennard-Jones 12-10 potential. The Dreiding forcefield has good coverage for organic, biological and main-group inorganic molecules. It is only moderately accurate for geometries, conformational energies, intermolecular binding energies and crystal packing [42].

The atom-based summation method with cut-off radii of 12.5 Å and long range corrections was used in calculation of the vdW interactions. The electrostatic interactions were dealt with via the Ewald [43] summation method with the accuracy of 10^{-5} kcal/mol.

4. SIMULATION DETAILS

The C-O bond in epoxide groups need to be broken in order to form a reactive -CH₂ site, capable of being cross-linked to DETA molecule (Fig. 2).



Fig. 2 – Conversion of an original epoxide group to a reactive one through breaking the C-O bond

The cross linking procedure, presented in our previous study [44], was used to create a representative cross-linked epoxy chain, composed of one DETA and four DGEBA molecules. The Amorphous Cell builder module of Materials Studio was then employed to construct four simulation cells, including 30 representative cross-linked chains, based on the above mentioned force fields. All cells were built at room temperature and atmospheric pressure, with the initial density of 0.5 g/cm³. Fig. 3 illustrates an example of the constructed epoxy amorphous cells.

The systems were subjected to energy minimization using the combination of steepest descent and conjugate gradient (Fletcher-Reeves) algorithms, to reach the nearest local minimum.

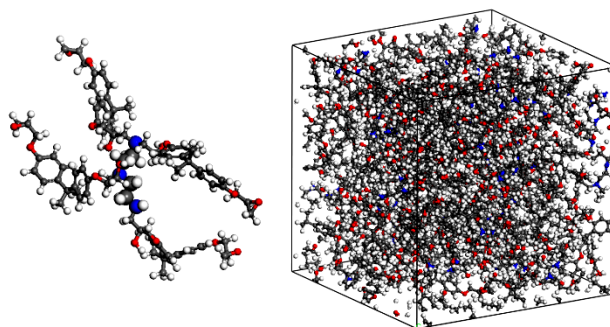


Fig. 3 – Representative cross-linked epoxy chain (left), and amorphous cell composed of 30 epoxy chains

Thereafter, 500 ps isothermal-isobaric (NPT) dynamics with time step of 1 fs at 298 K and 1 atm was

performed in order to equilibrate the systems and reach the real density. The Berendsen thermostat and barostat were used to control, respectively, the temperature and pressure of the system during the simulation. The time evolutions of the potential energy, temperature and density of the system were monitored during the dynamics, and the equilibrium state was confirmed as they got stable with slight fluctuations around constant values.

5. MECHANICAL PROPERTIES

There are three main approaches, static (constant-strain minimization) [45], dynamics (constant-stress molecular dynamics) [46, 47], and fluctuation formula [48-50], for calculation of the mechanical properties using MD simulations.

The static method was used in current study to estimate the mechanical properties of the cross-linked epoxy polymer, via different force fields.

In the case of linear elastic materials, the stress-strain behavior can be described by generalized Hooke's law. Considering the symmetry of the stress, strain and stiffness tensors, the number of independent components in the stiffness tensor would be reduced from 81 to 21, and hence, the Hooke's law can be written in a second-order form, using Voigt notation as:

$$\sigma_i = C_{ij}\varepsilon_j \quad (1)$$

where $i, j = 1, 2, 3$. σ_i and ε_i are the 6-dimensional stress and strain vectors, respectively, and C_{ij} is the 6×6 stiffness matrix.

Calculation of the mechanical properties was initiated by pre-minimization of the structure, to make sure that the calculations are based on the most stable configuration. The minimized structure was strained under a set of 12 deformations (three pairs of uniaxial tension/compression and three pairs of pure shear), controlled by the corresponding strain vectors, with one component taking a tiny value, while the others kept fixed at zero, and then re-minimized without any change in cell parameters. The maximum strain amplitude was set to ± 0.003 .

The stress components were calculated using the so-called virial expression:

$$\sigma_{ij} = -\frac{1}{V} \sum_k \left(m^k (u_i^k u_j^k) + \frac{1}{2} \sum_{l \neq k} (r_i^{kl} f_j^{lk}) \right) \quad (2)$$

with the first term on the right hand side omitted because of the static conditions. Here, V is the volume, m^k and u^k denote the mass and velocity of the k^{th} particle, respectively, r^{kl} stands for the distance between k^{th} and l^{th} particles, and f^{lk} is the force exerted on l^{th} particle by k^{th} particle. The elastic stiffness constants were then obtained using the first derivative of the virial stress with respect to the strain, $\partial\sigma / \partial\varepsilon$. In other words, the full 6×6 stiffness matrix was built up from the slopes $\partial\sigma / \partial\varepsilon$ in tension and shear.

Lamé coefficients, λ and μ , can be calculated using any two of the following equations:

$$\lambda = \frac{1}{6} (C_{12} + C_{13} + C_{21} + C_{23} + C_{31} + C_{32}) \quad (3a)$$

$$\approx \frac{1}{3} (C_{12} + C_{23} + C_{13})$$

$$\mu = \frac{1}{3} (C_{44} + C_{55} + C_{66}) \quad (3b)$$

$$\lambda + 2\mu = \frac{1}{3} (C_{11} + C_{22} + C_{33}) \quad (3c)$$

The other material properties can be simply calculated from the Lamé coefficients, as follows:

$$E = \frac{\mu(3\lambda + 2\mu)}{\lambda + \mu} \quad (4a)$$

$$K = \lambda + \frac{2}{3}\mu \quad (4b)$$

$$G = \mu \quad (4c)$$

$$\nu = \frac{\lambda}{2(\lambda + \mu)} \quad (4d)$$

where E, K and G stand for Young's, bulk and shear moduli, respectively, and ν denotes the Poisson's ratio.

6. RESULTS AND DISCUSSION

The variation of density with respect to simulation time for all four models is depicted in Fig. 4.

The 6×6 elastic stiffness matrix for cross-linked epoxy was calculated based on different force fields, as follow:

COMPASS:

$$C_{ij} = \begin{pmatrix} 4.68 & 2.13 & 1.95 & 0.01 & 0.01 & -0.07 \\ 2.13 & 5.25 & 2.49 & -0.01 & 0.06 & 0.01 \\ 1.95 & 2.49 & 5.11 & -0.20 & 0.06 & -0.09 \\ 0.01 & -0.01 & -0.20 & 1.30 & -0.07 & 0.03 \\ 0.01 & -0.83 & 0.06 & 0.06 & -0.07 & 1.25 \\ -0.07 & 0.01 & -0.09 & 0.03 & 0.04 & 1.35 \end{pmatrix}$$

PCFF:

$$C_{ij} = \begin{pmatrix} 4.52 & 2.37 & 2.38 & -0.10 & -0.03 & 0.05 \\ 2.37 & 4.82 & 2.43 & -0.12 & 0.03 & 0.10 \\ 2.38 & 2.43 & 4.71 & 0.08 & -0.28 & 0.06 \\ -0.10 & -0.12 & 0.08 & 1.09 & 0.11 & -0.02 \\ -0.03 & 0.03 & -0.28 & 0.11 & 1.24 & 0.03 \\ 0.05 & 0.10 & 0.06 & -0.02 & 0.03 & 1.23 \end{pmatrix}$$

UFF:

$$C_{ij} = \begin{pmatrix} 5.51 & 2.50 & 1.79 & 0.32 & -0.24 & -0.08 \\ 2.50 & 5.64 & 2.23 & 0.26 & -0.08 & -0.46 \\ 1.79 & 2.23 & 5.24 & 0.11 & 0.21 & -0.30 \\ 0.32 & 0.26 & 0.11 & 1.61 & -0.06 & -0.02 \\ -0.24 & -0.08 & 0.21 & -0.06 & 1.84 & -0.08 \\ 0.08 & -0.46 & -0.30 & -0.02 & -0.09 & 1.60 \end{pmatrix}$$

Dreiding:

$$C_{ij} = \begin{pmatrix} 3.01 & 1.34 & 1.22 & -0.21 & -0.18 & -0.35 \\ 1.34 & 3.23 & 1.09 & 0.08 & -0.34 & -0.27 \\ 1.22 & 1.09 & 3.12 & -0.28 & -0.09 & -0.14 \\ -0.21 & 0.08 & -0.28 & 0.59 & 0.03 & -0.07 \\ -0.18 & -0.34 & -0.09 & 0.03 & 0.89 & -0.04 \\ -0.35 & -0.27 & -0.14 & -0.07 & -0.04 & 1.01 \end{pmatrix}$$

The estimated mechanical properties for all four models are provided in Table 1, beside some experimental values.

As can be seen, there is excellent agreement between the COMPASS-based results and experimental data. PCFF-based results are quite accurate, as well. Results achieved from UFF and Dreiding are moderately reasonable.

Table 1 – Mechanical properties of the cross-linked epoxy from MD simulations, using different force fields, in comparison with experimental data (all moduli are in GPa)

Property	Simulations results				Experimental results
	Compass	PCFF	UFF	Dreiding	
Young's modulus, E	3.44	3.16	4.30	2.19	3.05 – 3.86 [51-53]
Shear modulus, G	1.3	1.19	1.68	0.83	–
Bulk modulus, K	3.28	3.10	3.22	2.01	–
Poisson's ratio, ν	0.32	0.33	0.28	0.32	0.36 ± 0.06 [53]
Density, g/cm ³	1.11	1.08	1.05	0.91	1.16 [51], 1.19 [54]

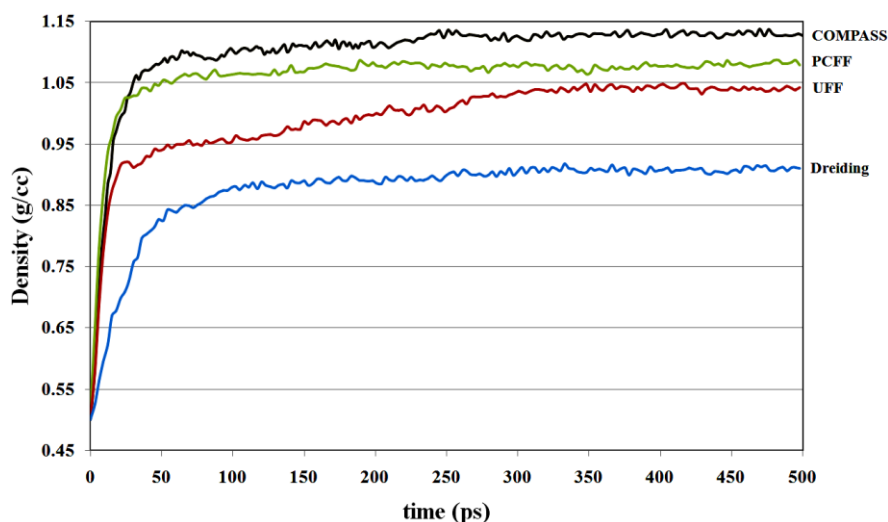


Fig. 4 – Equilibration of the density using different force fields through 500 ps NPT dynamics

7. CONCLUSIONS

In this study, the molecular dynamics with COMPASS, PCFF, UFF and Dreiding force fields was successfully utilized for calculation of the material properties of cross-linked epoxy polymers using the constant

strain (static) approach. The simulation results revealed that the COMPASS and PCFF with can be reliably used for simulation of cross-linked polymers and calculation of their properties. UFF- and Dreiding-based results would be relatively reasonable.

REFERENCES

- J.P. Pascault, R.J.J. Williams, *Epoxy Polymers: New Materials and Innovations* (Weinheim: Wiley-VCH: 2010).
- D.C. Doherty, B.N. Holmes, P. Leung, R.B. Ross, *Comput. Theor. Polym. Sci.* **8**,169 (1998).
- M. Tsige, M.J. Stevens, *Macromolecules* **37**, 630 (2004).
- J.S. Bermejo, C.M. Ugarte, *Macromol. Theor. Simul.* **18**, 259 (2009).
- J.S. Bermejo, C.M. Ugarte, *Macromol. Theor. Simul.* **18**, 317 (2009).
- O. Hölck, E. Dermitzaki, B. Wunderle, J. Bauer, B. Michel, *Microelectron. Reliab.* **51**, 1027 (2011).
- A. Bandyopadhyay, P.K. Valavala, T.C. Clancy, K.E. Wise, G.M. Odegard, *Polymer* **52**, 2445 (2011).
- C. Li, A. Strachan, *Polymer* **51**, 6058 (2010).
- N. Nouri, S. Ziaei-Rad, *Macromolecules* **44**, 5481 (2011).
- J.L. Tack, D.M. Ford, *J. Mol. Graphics Modell.* **26**, 1269 (2008).
- V. Varshney, S.S. Patnaik, A.K. Roy, B.L. Farmer, *Macromolecules* **41**, 6837 (2008).
- J. Choi, S. Yu, S. Yang, M. Cho, *Polymer* **52**, 5197 (2011).
- H.B. Fan, M.M.F. Yuen, *Polymer* **48**, 2174 (2007).
- S. Yu, S. Yang, M. Cho, *Polymer* **50**, 945 (2009).
- S. Yu, S. Yang, M. Cho, *J. Appl. Phys.* **110**, 124302 (2011).
- H. Horstermann, R. Hentschke, M. Amkreutz, M. Hoffmann, M. Wirts-Rutters, *J. Phys. Chem. B* **114**, 17013 (2010).
- C. Wu, W. Xu, *Polymer* **47**, 6004 (2006).
- C. Wu, W. Xu, *Polymer* **48**, 5802 (2007).
- C. Wu, W. Xu, *Polymer* **48**, 5440 (2007).
- P.H. Lin, R. Khare, *Macromolecules* **42**, 4319 (2009).
- T. Clancy, S. Frankland, J. Hinkley, T. Gates, *Polymer* **50**, 2736 (2009).

22. A. Prasad, T. Grover, S. Basu, *Int. J. Eng. Sci. Technol.* **2** No 4, 17 (2010).
23. H. Liu, M. Li, Z.-Y. Lu, Z.-G. Zhang, C.-C. Sun, T. Cui, *Macromolecules* **44**, 8650 (2011).
24. S.-H. Chang, H.-S. Kim, *Polymer* **52**, 3437 (2011).
25. N.J. Soni, P.-H. Lin, R. Khare, *Polymer* **53**, 1015 (2012).
26. <http://accelrys.com/products/materials-studio/>.
27. D. Rigby, *Fluid Phase Equilib.* **217**, 77 (2004).
28. H. Sun, *Macromolecules* **26**, 5924 (1993).
29. S.W. Bunte, H. Sun, *J. Phys. Chem. B* **104**, 2477 (2000).
30. J. Fried, *Comput. Theor. Polym. S.* **8**, 229 (1998).
31. M.J. McQuaid, H. Sun, D. Rigby, *J. Comput. Chem.* **25**, 61 (2004).
32. J. Yang, Y. Ren, A. Tian, H. Sun, *J. Phys. Chem. B* **104**, 4951 (2000).
33. H. Sun, *J. Phys. Chem. B* **102**, 7338 (1998).
34. H. Sun, *J. Comput. Chem.* **15**, 752 (2004).
35. H. Sun, *Macromolecules* **28**, 701 (1995).
36. H. Sun, S.J. Mumby, J.R. Maple, A.T. Hagler, *J. Am. Chem. Soc.* **116**, 2978 (1994).
37. H. Sun, S. Mumby, J. Maple, A. Hagler, *J. Phys. Chem.* **99**, 5873 (1995).
38. A. Rappe, C. Casewit, K. Colwell, W. Goddard Iii, W. Skiff, *J. Am. Chem. Soc.* **114**, 10024 (1992).
39. A. Rappe, K. Colwell, C. Casewit, *Inorg. Chem.* **32**, 3438 (1993).
40. L. Castonguay, A. Rappe, *J. Am. Chem. Soc.* **114**, 5832 (1992).
41. S.L. Mayo, B.D. Olafson, W.A. Goddard, *J. Phys. Chem.* **94**, 8897 (1990).
42. *Online manual of Material Studio*, <http://accelrys.com/products/materials-studio/>.
43. P.P. Ewald, *Ann. Phys.* **369**, 253 (1921).
44. B. Arab, A. Shokuhfar, S. Ebrahimi-Nejad, *2nd International Conference – Nanomaterials: Application & Properties (NAP-2012)* **1**, 01NDLCN11 (Ukraine: Alushta: 2012).
45. D.N. Theodorou, U.W. Suter, *Macromolecules* **19**, 139 (1986).
46. H.J.C. Berendsen, J.P.M. Postma, W.F. Van Gunsteren, A. Dinola, J. Haak, *J. Chem. Phys.* **81**, 3684 (1984).
47. D. Brown, J.H.R. Clarke, *Macromolecules* **24**, 2075 (1991).
48. A.A. Gusev, M.M. Zehnder, U.W. Suter, *Phys. Rev. B* **54**, 1 (1996).
49. M. Parrinello, A. Rahman, *J. Chem. Phys.* **76**, 2662 (1982).
50. J.R. Ray, *Comput. Phys. Rep.* **8**, 109 (1988).
51. E. Brown, S. White, N. Sottos, *J. Mater. Sci.* **41**, 6266 (2006).
52. Y.C. Yuan, M.Z. Rong, M.Q. Zhang, J. Chen, G.C. Yang, X.M. Li, *Macromolecules* **41**, 5197 (2008).
53. G. Possart, M. Presser, S. Passlack, P. Geifl, M. Kopnarski, A. Brodyanski, P. Steinmann, *Int. J. Adhes. Adhes.* **29**, 478 (2009).
54. *EPON resin structural reference manual* (Texas: Shell Chemical Company: 1989).